

REPORT DOCUMENTATION PAGE			Form Approved OMB No. 0704-0188	
Public reporting burden for this collection of information is estimated to average 1 hour per response, including the time for reviewing instructions, searching existing data sources, gathering and maintaining the data needed, and completing and reviewing the collection of information. Send comments regarding this burden estimate or any other aspect of this collection of information, including suggestions for reducing this burden, to Washington Headquarters Services, Directorate for Information Operations and Reports, 1215 Jefferson Davis Highway, Suite 1204, Arlington, VA 22202-4302, and to the Office of Management and Budget, Paperwork Reduction Project (0704-0188), Washington, DC 20503.				
1. AGENCY USE ONLY (Leave blank)	2. REPORT DATE 31 Mar 2005	3. REPORT TYPE AND DATES COVERED REPRINT		
4. TITLE AND SUBTITLE Timescale for radiation belt electron acceleration by whistler mode chorus waves		5. FUNDING NUMBERS PE 62601F PR 1010 TA RS WU A1		
6. AUTHOR(S) Richard B. Horne*, Richard M. Thorne**, Sarah A. Glauert*, Jay M. Albert, Nigel P. Meredith#, and Roger R. Anderson##				
7. PERFORMING ORGANIZATION NAME(S) AND ADDRESS(ES) Air Force Research Laboratory/VSBX 29 Randolph Road Hanscom AFB, MA 01731-3010		8. PERFORMING ORGANIZATION REPORT NUMBER AFRL-VS-HA-TR-2005-1079		
9. SPONSORING/MONITORING AGENCY NAME(S) AND ADDRESS(ES)		10. SPONSORING/MONITORING AGENCY REPORT NUMBER		
11. SUPPLEMENTARY NOTES Reprinted from: J. Geophysical Res., Vol. 110, A03225, doi:10.1029/2004JA010811, 2005. Copyright 2005 by the American Geophysical Union. *British Antarctic Survey, Cambridge, UK. **Univ. of California, Los Angeles, CA. (Continued)				
12a. DISTRIBUTION AVAILABILITY STATEMENT Approved for public release; distribution unlimited.		12b. DISTRIBUTION CODE		
13. ABSTRACT (Maximum 200 words) Electron acceleration inside the Earth's magnetosphere is required to explain increases in the ~MeV radiation belt electron flux during magnetically disturbed periods. Recent studies show that electron acceleration by whistler mode chorus waves becomes most efficient just outside the plasmapause, near L = 4.5, where peaks in the electron phase space density are observed. We present CRRES data on the spatial distribution of chorus emissions during active conditions. The wave data are used to calculate the pitch angle and energy diffusion rates in three magnetic local time (MLT) sectors and to obtain a timescale for acceleration. We show that chorus emissions in the prenoon sector accelerate electrons most efficiently at latitudes above 15° for equatorial pitch angles between 20° and 60°. As electrons drift around the earth, they are scattered to large pitch angles and further accelerated by chorus on the nightside in the equatorial region. The timescale to accelerate electrons by whistler mode chorus and increase the flux at 1 MeV by an order of magnitude is approximately 1 day, in agreement with satellite observations during the recovery phase of storms. During wave acceleration the electrons undergo many drift orbits and the resulting pitch angle distributions are energy-dependent. Chorus scattering should produce pitch angle distributions that are either flat-topped or butterfly-shaped. The results provide strong support for the wave acceleration theory.				
14. SUBJECT TERMS Chorus waves Quasilinear diffusion Radiation belt electrons		15. NUMBER OF PAGES		
		16. PRICE CODE		
17. SECURITY CLASSIFICATION OF REPORT UNCL	18. SECURITY CLASSIFICATION OF THIS PAGE UNCL	19. SECURITY CLASSIFICATION OF ABSTRACT UNCL	20. LIMITATION OF ABSTRACT UNL	

Timescale for radiation belt electron acceleration by whistler mode chorus waves

Richard B. Horne,¹ Richard M. Thorne,² Sarah A. Glauert,¹ Jay M. Albert,³ Nigel P. Meredith,^{4,5} and Roger R. Anderson⁶

Received 28 September 2004; revised 25 November 2004; accepted 13 January 2005; published 31 March 2005.

[1] Electron acceleration inside the Earth's magnetosphere is required to explain increases in the \sim MeV radiation belt electron flux during magnetically disturbed periods. Recent studies show that electron acceleration by whistler mode chorus waves becomes most efficient just outside the plasmapause, near $L = 4.5$, where peaks in the electron phase space density are observed. We present CRRES data on the spatial distribution of chorus emissions during active conditions. The wave data are used to calculate the pitch angle and energy diffusion rates in three magnetic local time (MLT) sectors and to obtain a timescale for acceleration. We show that chorus emissions in the prenoon sector accelerate electrons most efficiently at latitudes above 15° for equatorial pitch angles between 20° and 60° . As electrons drift around the Earth, they are scattered to large pitch angles and further accelerated by chorus on the nightside in the equatorial region. The timescale to accelerate electrons by whistler mode chorus and increase the flux at 1 MeV by an order of magnitude is approximately 1 day, in agreement with satellite observations during the recovery phase of storms. During wave acceleration the electrons undergo many drift orbits and the resulting pitch angle distributions are energy-dependent. Chorus scattering should produce pitch angle distributions that are either flat-topped or butterfly-shaped. The results provide strong support for the wave acceleration theory.

Citation: Horne, R. B., R. M. Thorne, S. A. Glauert, J. M. Albert, N. P. Meredith, and R. R. Anderson (2005), Timescale for radiation belt electron acceleration by whistler mode chorus waves, *J. Geophys. Res.*, **110**, A03225, doi:10.1029/2004JA010811.

1. Introduction

[2] The flux of energetic electrons in the Earth's outer radiation belt can vary by 1000 fold or more during magnetic storms and other disturbances at the Earth driven by the Sun [Baker *et al.*, 1986, 1997, 1998a, 1998b]. These variations are due to a competition between acceleration and loss processes acting within the Earth's magnetic field [Li *et al.*, 1997; Baker *et al.*, 1989]. The flux variations are important since they have been associated with damage and loss of satellites at geostationary orbit [e.g., Baker *et al.*, 1998c; Baker, 2001; Horne, 2003]. Therefore to develop physics-based models to analyze and predict the Earth's radiation environment, it is important to understand the acceleration and loss processes.

[3] Several theories have been suggested to account for the acceleration (see the reviews by Li and Temerin [2001], Friedel *et al.* [2002], and Horne [2002]). For very rapid flux increases on timescales of minutes, shock acceleration has been suggested, since it can account for the very fast timescales [Hudson *et al.*, 1997]. However, these events are relatively unusual. Far more common are flux increases and decreases associated with magnetic storms [Reeves *et al.*, 2003] and periods of prolonged substorms [Meredith *et al.*, 2002a, 2003a], which have timescales for flux increase of the order of many hours to days.

[4] Betatron acceleration as a result of inward radial diffusion and conservation of the first adiabatic invariant is an important mechanism that operates inside the radiation belts [Schulz and Lanzerotti, 1974]. This mechanism can be enhanced by ULF waves [Elkington *et al.*, 1999]. However, there is increasing evidence from peaks in the phase space density [Brautigam and Albert, 2000; Green and Kivelson, 2004] and pitch angle distributions [Horne *et al.*, 2003a] that local acceleration by another mechanism is required in the heart of the outer radiation belt near $L \sim 4.5$. One of the most promising candidates is local acceleration by whistler mode waves through Doppler-shifted cyclotron resonance [Horne and Thorne, 1998; Summers *et al.*, 1998]. The model proposed is that substorms and inward radial diffusion provide a seed population of low-energy electrons. As they are injected to higher magnetic field strength, the distribution develops an anisotropy through conservation

¹British Antarctic Survey, Cambridge, UK.

²Department of Atmospheric Sciences, University of California, Los Angeles, California, USA.

³Space Vehicles Directorate, Air Force Research Laboratory, Hanscom Air Force Base, Massachusetts, USA.

⁴Mullard Space Science Laboratory, University College London, Dorking, UK.

⁵Also at British Antarctic Survey, Cambridge, UK.

⁶Department of Physics and Astronomy, University of Iowa, Iowa City, Iowa, USA.

of the first two adiabatic invariants and excites whistler mode waves. These waves accelerate the particles by transferring energy from low-energy electrons at small pitch angles to high-energy electrons at large pitch angles through Doppler-shifted cyclotron resonance. Indeed, several studies have shown that relativistic electron flux enhancements are associated with prolonged substorm activity, an elevated flux of seed electrons, and prolonged periods of enhanced chorus amplitudes lasting for the order of several days [Meredith *et al.*, 2002a, 2003a; Miyoshi *et al.*, 2003]. A recent statistical analysis of magnetically disturbed periods suggests that radial diffusion is efficient in the outer magnetosphere, whereas local acceleration may dominate in the inner magnetosphere [O'Brien *et al.*, 2003].

[5] In order for whistler mode acceleration to be viable, waves must be able to accelerate the electrons on timescales consistent with observations. While previous estimates have generally been favorable, they have assumed field-aligned waves [Summers *et al.*, 2002, 2004] and a uniform distribution of wave power in magnetic local time (MLT) [Horne *et al.*, 2003b]. Another factor that is critical to the efficiency of wave acceleration is the ratio of the electron plasma frequency to the electron gyrofrequency f_{pe}/f_{ce} [Summers *et al.*, 1998; Horne *et al.*, 2003b]. Whistler mode acceleration is more efficient in regions of low density, since this increases the phase velocity of the waves for the dominant cyclotron resonance. Observations show that whistler mode wave power and f_{pe}/f_{ce} vary considerably with magnetic activity, L , MLT, and magnetic latitude λ_m [Meredith *et al.*, 2003c]. The purpose of this paper is to take these variations into account by analyzing data from the CRRES satellite in different MLT sectors and constructing models to calculate the timescale for electron acceleration on a global scale. To accomplish this, we have developed new pitch angle and energy diffusion codes that are not restricted to the high plasma density approximation made in previous codes but can also treat diffusion in the low-density limit [Glauert and Horne, 2005; Albert, 2005]. We find that wave acceleration is very dependent on magnetic local time and latitude, but the resulting timescale should be sufficient to increase the \sim MeV electron flux by an order of magnitude at $L \approx 4.5$ within 24 hours, consistent with observations.

2. Data Distribution in MLT

[6] Using data from the Combined Release and Radiation Effects Satellite (CRRES), we constructed a database to study the spatial distribution of whistler mode wave power and the ratio f_{pe}/f_{ce} . CRRES operated in an elliptical geosynchronous transfer orbit with a perigee of 305 km, apogee of 35,768 km, and inclination of 18° . The orbital period was approximately 10 hours, and the mission lasted for almost 15 months. Thus during the mission lifetime, the satellite sampled all MLT through the radiation belts. The data used in this study were taken from the Plasma Wave Experiment, which measured electric fields between 5.6 Hz and 400 kHz [Anderson *et al.*, 1992], and the fluxgate magnetometer [Singer *et al.*, 1992]. Since pitch angle and energy diffusion rates scale as the power of the wave magnetic field, the electric field spectral intensity, S_E , was converted into magnetic field spectral intensity, S_B , by using Faraday's law and the cold plasma dispersion relation for

wave propagation parallel to the ambient magnetic field B_0 [Stix, 1992, p. 26], given by

$$S_B = \frac{1}{c^2} \left(1 - \frac{f_{pe}^2}{f(f - f_{ce})} \right) S_E, \quad (1)$$

where c is the speed of light and f is the wave frequency. The plasma frequency was determined from observations of electrostatic waves at the local upper hybrid frequency f_{UHR} and from the lower-frequency cutoff of electromagnetic continuum radiation, as described by Meredith *et al.* [2002a]. The magnetic field wave amplitude was obtained by integrating the average wave spectral density ($\text{pT}^2 \text{Hz}^{-1}$) over frequency and taking the square root. The data were sampled and binned in steps of 0.1L. The L shell and magnetic latitude λ_m were obtained from the Olsen-Pfizer magnetic field model [Olsen and Pfizer, 1977].

[7] The distribution of chorus wave amplitudes with f_{pe}/f_{ce} have been presented for different levels of substorm activity before [Meredith *et al.*, 2003c]. The previous studies used the level of substorm activity, as measured by the AE index, and selected data for $AE > 300$ nT as the highest level of substorm activity. They also limited the frequency band to $0.1f_{ce} < f < 0.5f_{ce}$. However, since diffusion rates are sensitive to the peak wave power and, as we shall show, are sensitive to lower normalized frequencies at high latitudes, we have reanalyzed the CRRES data for $AE > 500$ nT, and $f_{LHR} < f < 0.5f_{ce}$, where f_{LHR} is the lower hybrid resonance frequency. Therefore in this paper we define lower-band chorus as chorus in the frequency range $f_{LHR} < f < 0.5f_{ce}$ and not $0.1f_{ce} < f < 0.5f_{ce}$ used in previous studies.

[8] The average lower-band chorus amplitudes during active conditions are shown as a function of L and MLT for the equatorial and midlatitude regions in the top panels of Figure 1. The analysis is restricted to lower-band chorus since these waves resonate with \sim MeV electrons and since lower-band chorus is generally stronger than upper-band chorus [Meredith *et al.*, 2001, 2002b]. In the equatorial region (top left), defined here as waves between $-15^\circ < \lambda_m < 15^\circ$, chorus wave amplitudes are enhanced from just before midnight, through dawn, to about 1200 MLT. Wave amplitudes are enhanced for $3 < L < 6$ and can exceed 100 pT. Unfortunately, there are very few samples in the 0900–1200 MLT sector. The region of enhanced wave amplitudes also corresponds to regions where f_{pe}/f_{ce} is typically less than 4 (bottom left), indicating that the region from midnight through dawn should contribute to wave acceleration. In comparison to equatorial chorus, midlatitude chorus (between $15^\circ < |\lambda_m| < 30^\circ$) is enhanced on the dayside between 0600 and 1500 MLT. The emissions before 1200 MLT are associated with low values of f_{pe}/f_{ce} , typically less than 3, and thus should also contribute to wave acceleration. However, at night there is very little wave power at high latitudes even though the ratio f_{pe}/f_{ce} is smaller. The data show that there are substantial differences in wave amplitudes and f_{pe}/f_{ce} with MLT, and thus there should be substantial differences in the pitch angle and energy diffusion rates.

[9] To take into account MLT effects on the diffusion rates, we have averaged the CRRES data into three local time sectors, where in each sector the data exhibit similar

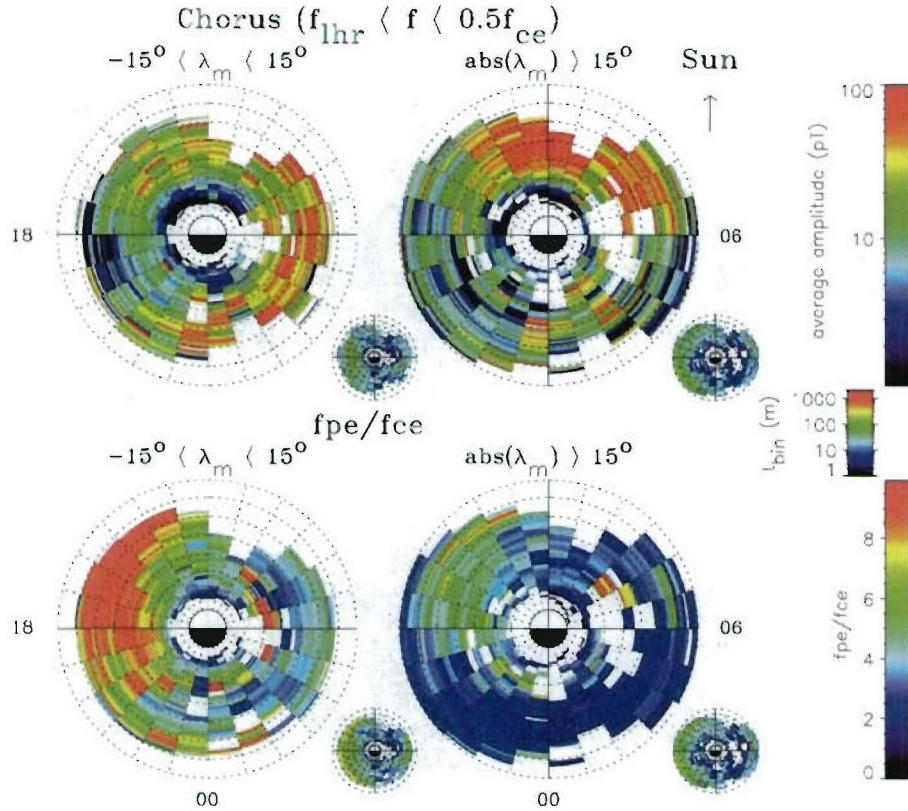


Figure 1. Magnetic local time (MLT) dependence of (top) chorus wave amplitudes and (bottom) the electron plasma to gyro frequencies f_{pe}/f_{ce} . The data are for high substorm activity $AE > 500$ nT, for the (left) equatorial and (right) midlatitude regions. The insets show the time spent sampling each $0.1L$ bin.

variations in wave power and latitude. The MLT sectors are referred to as night (2300–0600 MLT), prenoon (0600–1200 MLT), and afternoon (1200–1500 MLT). The remaining MLT sector is not included, since the wave power is low and f_{pe}/f_{ce} is high so that no significant acceleration is expected. The data are restricted to $L = 4.5 \pm 0.5L$, corresponding to the approximate peak in electron phase space density during the recovery period of magnetic storms [Green and Kivelson, 2004]. All the data are for a high level of substorm activity, $AE > 500$ nT, and data for southern latitudes has been averaged with northern latitudes to improve the statistics. Figure 2 shows the results for the median (solid), upper, and lower (dashed) quartiles of the average wave amplitude for $f_{LHR} < f < 0.5 f_{ce}$ (top) and ratio f_{pe}/f_{ce} (bottom).

[10] Chorus wave amplitudes peak around 50 pT for $\lambda_m < 15^\circ$ in the night MLT sector and decrease with increasing latitude (top left). On the other hand, wave amplitudes increase with latitude in the prenoon sector, reaching a maximum around $\lambda_m \approx 25^\circ$. The prenoon sector has the largest wave amplitudes of all the MLT shown. In the afternoon sector, wave amplitudes also tend to increase with increasing latitude but are generally smaller than prenoon. The ratio f_{pe}/f_{ce} generally decreases with increasing latitude in each MLT sector. However, f_{pe}/f_{ce} is smaller in the night sector. The data for f_{pe}/f_{ce} are more variable in the prenoon and afternoon sectors, probably due to a time

delay between the increase in AE above 500 nT and the motion of the high-density plasmopause.

[11] Using the data, we have constructed three models for the variation in wave amplitude and plasma density corresponding to each MLT sector at $L = 4.5$. We have restricted the magnetic field variations to a dipole and kept the plasma density constant with latitude. The wave power in each model is kept constant to reduce the complexity of the calculations and to help physical interpretation. The models are overlaid in Figure 2 (long dashed lines).

[12] For the night model, $f_{pe}/f_{ce} = 3.43$ at the magnetic equator and the average wave magnetic field amplitude is $B_w = 50$ pT over a latitude range $|\lambda_m| < 15^\circ$. The wave amplitude is zero outside this range. For the prenoon model, $f_{pe}/f_{ce} = 4.0$ at the equator and $B_w = 100$ pT for $15^\circ < |\lambda_m| < 35^\circ$. This gives a reasonable variation over the latitude region where the wave power peaks, for example, $f_{pe}/f_{ce} = 1.8$ at $\lambda_m = 25^\circ$. For the afternoon model, $f_{pe}/f_{ce} = 6.72$ at the equator and $B_w = 50$ pT for $10^\circ < |\lambda_m| < 35^\circ$.

3. Diffusion Model

[13] Following previous methods [Lyons *et al.*, 1972; Lyons, 1974; Albert, 1999], we calculate the bounce-averaged diffusion coefficients for equatorial pitch angle $\langle D_{\alpha_{eq}\alpha_{eq}} \rangle$, mixed pitch angle momentum $\langle D_{\alpha_{eq}p} \rangle$, and momentum $\langle D_{pp} \rangle$ in the fully relativistic limit. The bounce-

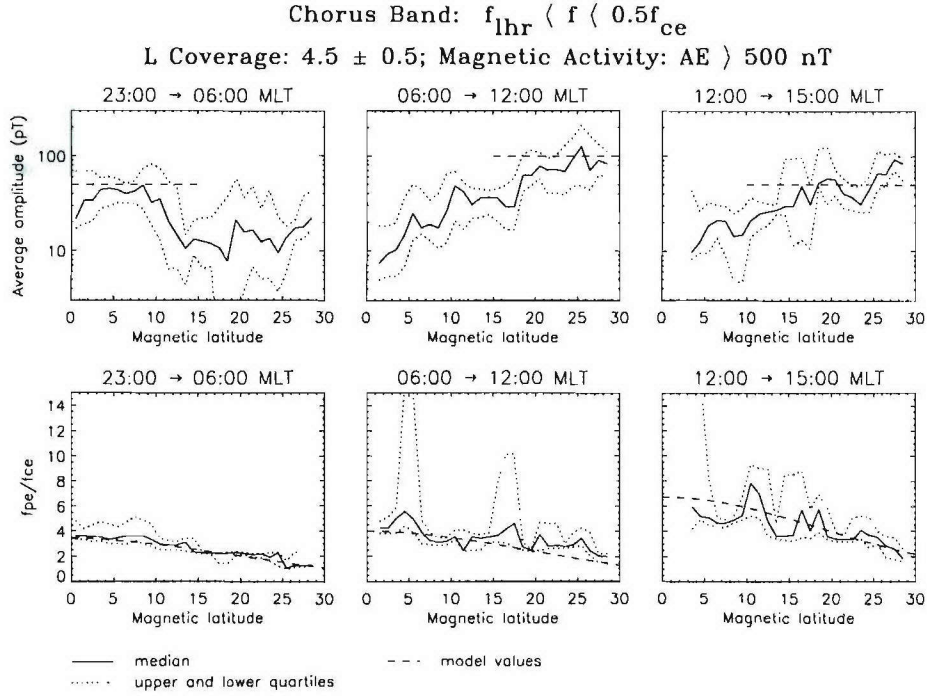


Figure 2. (top) Average chorus wave amplitudes and (bottom) ratio f_{pe}/f_{ce} for different magnetic local time sectors, (left) night, (middle) prenoon, and (right) afternoon, for $AE > 500$ nT at $L = 4.5$. Data for southern and northern latitudes are averaged together. The median, upper, and lower quartiles are shown by the solid and short dashed lines, respectively. The model values are shown by the long dashed lines.

averaged diffusion coefficients are obtained by bounce-averaging the relativistic quasi-linear diffusion equation, given by [Lyons and Williams, 1984, p. 140]

$$\begin{aligned} \frac{\partial f_0}{\partial t} &= \nabla \cdot (\mathbf{D} \cdot \nabla f_0) \\ &= \frac{1}{p^2 \sin \alpha} \frac{\partial}{\partial \alpha} p \sin \alpha \left(D_{\alpha\alpha} \frac{1}{p} \frac{\partial f_0}{\partial \alpha} + D_{\alpha p} \frac{\partial f_0}{\partial p} \right) \\ &\quad + \frac{1}{p^2} \frac{\partial}{\partial p} p^2 \left(D_{p\alpha} \frac{1}{p} \frac{\partial f_0}{\partial \alpha} + D_{pp} \frac{\partial f_0}{\partial p} \right), \end{aligned} \quad (2)$$

where α is the particle pitch angle ($\tan \alpha = p_{\perp}/p_{\parallel}$), $f_0(\mathbf{p}, t)$ is the zero-order spatially uniform particle distribution function for the species σ , with charge q_{σ} , and rest mass $m_{0\sigma}$, and $D_{\alpha\alpha}$, $D_{\alpha p}$ and D_{pp} are the local diffusion coefficients defined as

$$D_{\alpha\alpha} = \frac{p^2 \langle (\Delta \alpha)^2 \rangle}{2 \Delta t} \quad (3)$$

$$D_{\alpha p} = \frac{p \langle \Delta \alpha \Delta p \rangle}{2 \Delta t} \quad (4)$$

$$D_{pp} = \frac{\langle (\Delta p)^2 \rangle}{2 \Delta t}. \quad (5)$$

It is important to note that the diffusion rates have dimensions of momentum² s⁻¹. However, in the results below, we divide by p^2 to give the diffusion rates in s⁻¹. The energy $\langle D_{EE} \rangle$ and mixed pitch angle energy $\langle D_{\alpha E} \rangle$

diffusion rates are obtained from the momentum diffusion rates and divided by E^2 to obtain the same units of s⁻¹.

[14] While previous work uses the high-density approximation for whistler mode dispersion, we use the full dispersion relation. This enables us to address diffusion in low and high plasma densities but increases the mathematical complexity significantly. The results have been obtained and checked by two new and independent codes. Both use the full cold plasma dispersion relation, but one (PADIE) solves a high-order polynomial to obtain all possible resonant frequencies and then selects those corresponding to the whistler branch [Glauert and Horne, 2005], while the other uses the properties of the whistler mode to find the resonances within the specified range of frequency and wavenormal angles [Albert, 2005].

[15] To calculate the diffusion coefficients, the total wave power, frequency distribution, and angular distribution of wave power must be specified. The frequency distribution is assumed to be Gaussian, given by

$$B^2(\omega) = A^2 \exp \left[- \left(\frac{\omega - \omega_m}{\delta \omega} \right)^2 \right], \quad (6)$$

where $B^2(\omega)$ is the power spectral density of the wave magnetic field (in nT² Hz⁻¹), ω_m and $\delta \omega$ are the frequency of maximum wave power and bandwidth, respectively (in radians s⁻¹), and

$$A^2 = \frac{|B_w|^2}{\delta \omega} \frac{2}{\sqrt{\pi}} \left(\operatorname{erf} \left(\frac{\omega_m - \omega_{lc}}{\delta \omega} \right) + \operatorname{erf} \left(\frac{\omega_{lc} - \omega_m}{\delta \omega} \right) \right)^{-1}. \quad (7)$$

B_w is in units of nT. The wave spectrum is also bounded by upper ω_{uc} and lower ω_{lc} frequency limits and is zero outside these limits. We also assume that the wave power is spread over a Gaussian distribution of wave normal angles ψ given by

$$g_w(X) = \exp \left[- \left(\frac{X - X_m}{X_w} \right)^2 \right], \quad (8)$$

where $X = \tan \psi$, X_w is the angular width and X_m is the peak. The derivation of the diffusion coefficients, and methods of computation, are given in full elsewhere [Glauert and Horne, 2005; Albert, 2005].

[16] Since growth rates for whistler mode waves maximize for parallel propagation, for each model we assume that the wave power peaks in the field-aligned direction, $X_m = 0$, with an angular distribution of $\Delta\psi = 30^\circ$ ($X_w = 0.577$). At each frequency the wave power is integrated from $X = 0$ to $X = 1$ (or up to the resonance cone angle if that is smaller). Since wave propagation at an angle to the magnetic field is included, we calculate the diffusion rates for Landau ($n = 0$) and ± 1 cyclotron harmonic resonances.

4. Bounce-Averaged Diffusion Rates

[17] The bounce-averaged pitch angle and energy diffusion rates for the night model are shown in Figure 3. For the night model we assume that the wave amplitude peaks at $\omega_m = 0.35\Omega_e$ and has a bandwidth $\delta\omega = 0.15\Omega_e$, typical of lower-band chorus emissions [e.g., Meredith et al., 2001]. The lower and upper cutoff frequencies are set to $\omega_{lc} = 0.05\Omega_e$ and $\omega_{uc} = 0.65\Omega_e$, respectively. The momentum diffusion rates $\langle D_{pp} \rangle$ have been converted into energy diffusion rates $\langle D_{EE} \rangle$.

[18] The very narrow peaks in the diffusion rates near 80° correspond to diffusion by individual resonances, particularly the $n = 0$ Landau and $n = \pm 1$ cyclotron resonances. The higher-order resonances occur at smaller pitch angles and add in such a way as to give a smoother profile. The largest pitch angle diffusion rates occur at energies of ~ 30 keV. At low energies, pitch angle diffusion maximizes at small pitch angles and thus electron scattering into the loss cone is very effective. Energy diffusion maximizes for $\alpha_{eq} < 60^\circ$ (bottom) and thus for any moderate loss cone anisotropy, 30 keV electrons contribute the most to whistler mode wave growth as they are scattered to smaller pitch angles. At higher energies, pitch angle diffusion is reduced at small pitch angles and peaks between 60° and 80° . This indicates that pitch angle diffusion is most effective at large angles but that the particles remain trapped in the magnetosphere, typically for periods of several days for $E > 300$ keV. These trapped particles can undergo significant energy diffusion. For example, assuming a separation of variables, pitch angle and energy, in the diffusion equation, the timescale τ_E for electrons to diffuse in energy by a factor of e (2.718) by pure energy diffusion can be estimated from the inverse of the energy diffusion coefficient. Thus the energy diffusion timescale for 300 keV electrons is less than 13 hours.

[19] The net particle diffusion flux is toward lower phase space density. At large pitch angles and for a particle distribution function that has a modest anisotropy, the

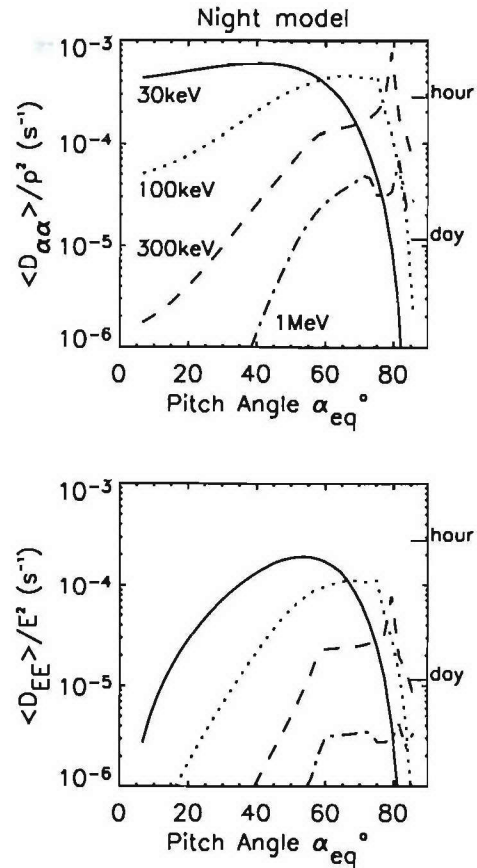


Figure 3. Bounce-averaged pitch angle $\langle D_{\alpha\alpha} \rangle$ and energy $\langle D_{EE} \rangle$ diffusion rates for whistler mode chorus waves as a function of equatorial pitch angle α_{eq} , for energies of 30, 100, 300, and 1000 keV, for the night model.

resonant diffusion surfaces along which the particles diffuse cut across the contours of the distribution function [e.g., Horne and Thorne, 2003, Figure 3]. Under these conditions, pitch angle diffusion at large pitch angles results in a net flux of particles toward higher energies and thus energy gain. Thus in Figure 3, there should be a net acceleration of particles at pitch angles more than $\sim 60^\circ$. In the absence of other source and loss processes, the diffusion should continue until the contours of the particle distribution function match the resonant diffusion surfaces. The net result is a transfer of energy from the large number of low-energy particles at ~ 30 keV, into the waves, and acceleration of a smaller number of >100 keV electrons at large pitch angles.

[20] In comparison to the night model, the diffusion rates for the prenoon model (Figure 4) show a different behavior. In the prenoon model the frequency of maximum wave power at the equator is larger, $\omega_m = 0.55\Omega_e$, in order to obtain the appropriate frequency band for chorus at higher latitudes $|\lambda_m| > 15^\circ$ where wave amplitudes maximize. The other parameters are $\delta\omega = 0.15\Omega_e$, $\omega_{lc} = 0.05\Omega_e$, and $\omega_{uc} = 0.95\Omega_e$. In this model all the diffusion rates drop rapidly for pitch angles greater than about 55° . This is due to our model assumption that there is no wave power at latitudes less than

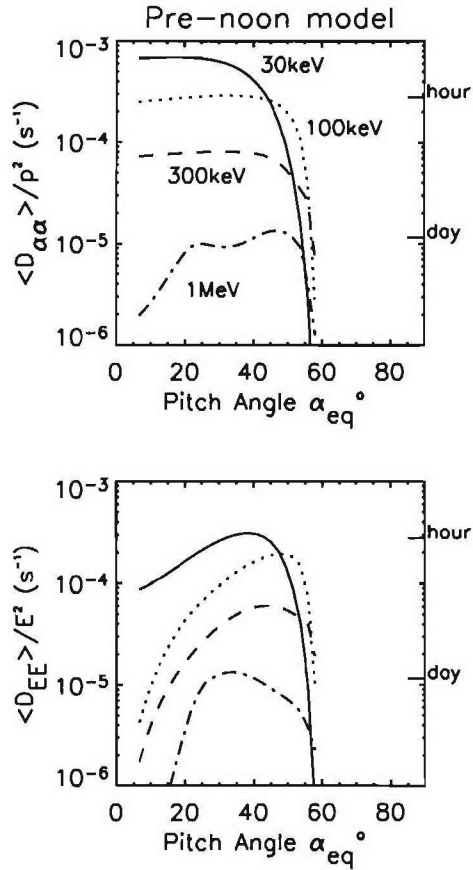


Figure 4. Bounce-averaged pitch angle $\langle D_{\alpha\alpha} \rangle$ and energy $\langle D_{EE} \rangle$ diffusion rates for whistler mode chorus waves as a function of equatorial pitch angle α_{eq} , for energies of 30, 100, 300, and 1000 keV, for the prenoon model.

15°, and thus when the diffusion rates are mapped back to the equator there is no scattering of the equatorial distribution function at pitch angles greater than 60°. Significant pitch angle scattering into the loss cone is possible for energies from 30 to 100 keV, with a timescale comparable to hour, but the losses become small for energies above 300 keV. In particular, at 1 MeV loss is insignificant, suggesting that once particles are accelerated to this energy they remain trapped for ~10 days. The largest energy diffusion (Figure 4, bottom) occurs for ~30 keV. The estimated timescale for acceleration 300 keV electrons is less than 5 hours but decreases with increasing energy to about 1 day at 1 MeV. The acceleration is only important for pitch angles between about 30° and 60° at these higher energies. Therefore the prenoon model alone does not produce acceleration all the way to 90°. In reality, there is wave power at low latitudes in the prenoon sector and so there will be some energy diffusion at large pitch angles. In addition, pitch angle diffusion is usually much larger than energy diffusion, and so, even though the power may be small near the equator, pitch angle diffusion will tend to smooth out any accelerated electrons so they should be seen near the equator.

[21] The diffusion rates for the afternoon model show a similar behavior to the prenoon model (Figure 5). In this

model $\omega_m = 0.45\Omega_e$, $\delta\omega = 0.15\Omega_e$, $\omega_{lc} = 0.05\Omega_e$, and $\omega_{uc} = 0.95\Omega_e$. The peak diffusion rates are smaller due to the lower wave amplitude 50 pT and are higher at larger pitch angles than the prenoon model due to wave power extending to lower latitudes. Clearly, while waves in this sector contribute to loss of low-energy electrons and acceleration, they are not as effective as the prenoon sector.

5. Global Diffusion Rates

[22] Energetic electrons drift around the Earth under the influence of the gradient and curvature drift and the convection electric field. However, for high energies the gradient and curvature drift are the most important factors. The drift periods of 0.1 to 1 MeV electrons at $L = 4.5$ in a dipole magnetic field lie between approximately 100 and 16 min, respectively. Thus during a storm recovery phase lasting a few days, electrons complete many drift orbits. During each drift orbit the particles will encounter waves in different MLT sectors and be scattered in pitch angle and energy. To take this into account, we have combined the results of the three models discussed above to obtain the drift average diffusion rates. We have multiplied the diffusion rates for each model by the fraction of MLT that the model represents, 7/24 for night, 6/24 for prenoon, and 3/24 for afternoon. The results are shown in Figure 6. The global

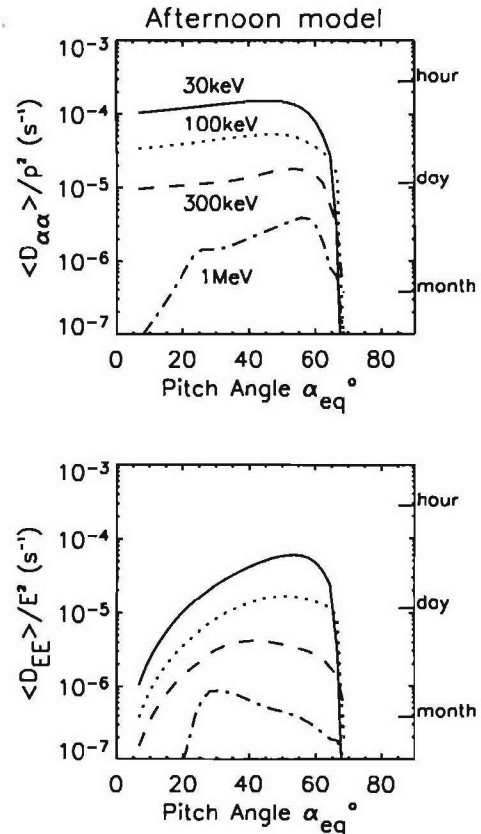


Figure 5. Bounce-averaged pitch angle $\langle D_{\alpha\alpha} \rangle$ and energy $\langle D_{EE} \rangle$ diffusion rates for whistler mode chorus waves as a function of equatorial pitch angle α_{eq} for energies of 30, 100, 300, and 1000 keV, for the afternoon model.

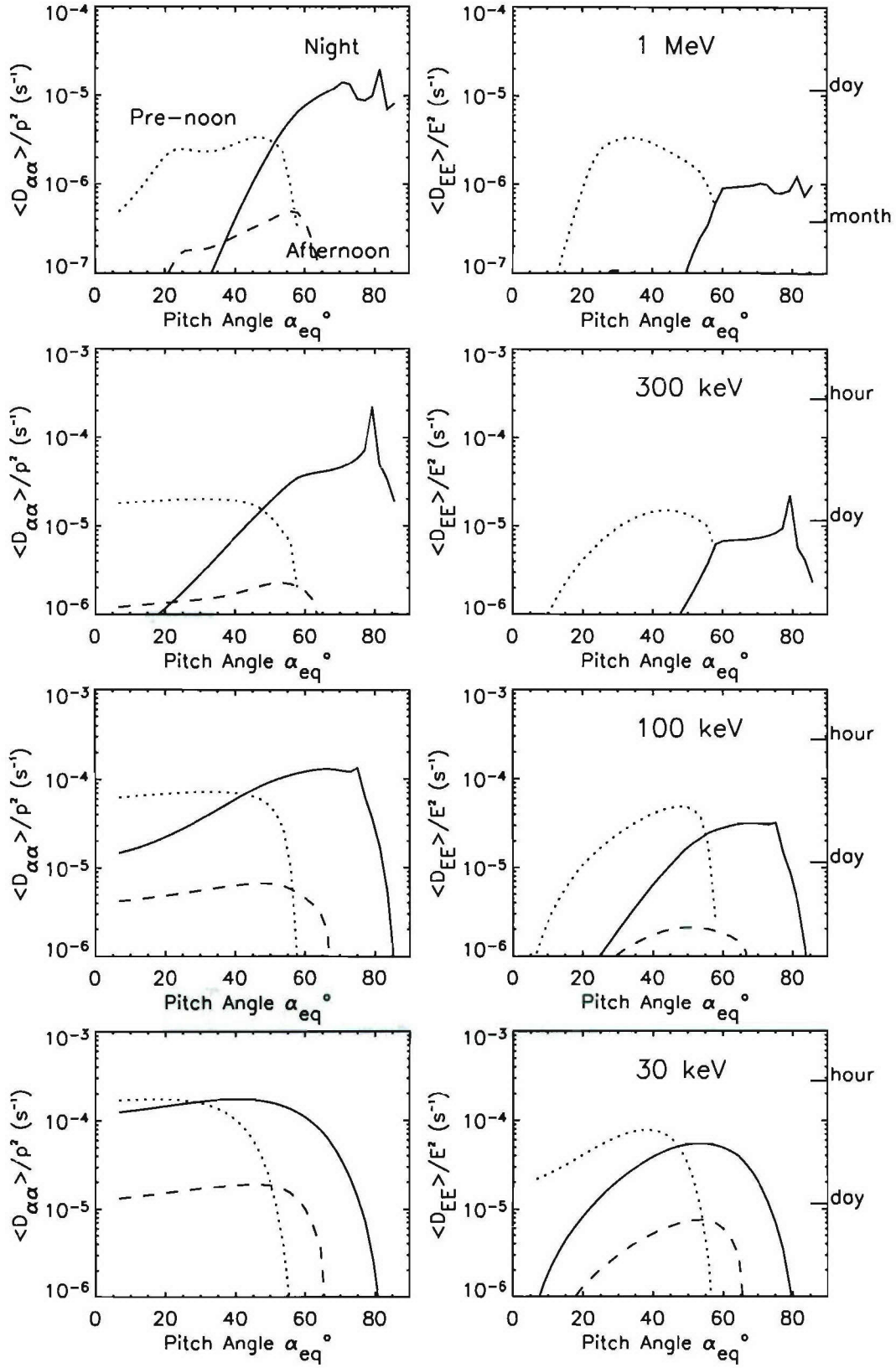


Figure 6. Bounce-averaged pitch angle and energy diffusion rates for whistler mode chorus waves for the night (solid), prenoon (dotted), and afternoon (dashed) models, weighted according to the MLT occurrence of the waves. The energies are, top to bottom, 1000, 300, 100, and 30 keV.

diffusion rate due to waves in all MLT sectors is therefore the sum of the diffusion rates shown in each panel in Figure 6. Thus it is clear that energy diffusion can extend to large pitch angles when the drift of the particles is taken into account.

[23] When the MLT occurrence of the waves is taken into account, only waves in the night and prenoon MLT sectors contribute significantly to particle diffusion. The diffusion rates generally decrease with increasing energy, but the key factor to emerge is that there is a competition between electron acceleration and electron loss that is energy dependent. By assuming a separation of variables and ignoring mixed pitch angle-energy diffusion, the timescale for electron loss can be estimated from the inverse of the pitch angle diffusion rate at the edge of the loss cone. At 30 keV, the loss timescale is approximately 2 hours. However, at 300 keV the loss and acceleration timescales are comparable at about 14 hours, but at 1 MeV the acceleration timescale becomes much shorter (3.9 days) than the loss timescale (23 days). The change in the timescales with energy is consistent with the concept of energy transfer, that as particles are diffused into the loss cone at low energies they give energy to the waves which accelerates particles at high energies. Since the timescale for loss at 30 keV is a few hours and since ~ 30 keV electrons are most likely to be responsible for the generation of chorus, a relatively continuous source of ~ 30 keV electrons is required for significant acceleration up to a few MeV. This suggests that prolonged substorm activity is a requirement for efficient acceleration.

6. Evolution of the Particle Flux

[24] The timescale estimates calculated above are for the evolution of the electron distribution function and not the particle flux that is usually measured by satellites. To compare with satellite observations, we first calculate the evolution of the distribution function from the diffusion equation and then convert this into an evolution of the electron flux. For this initial assessment we neglect the mixed pitch angle-energy diffusion coefficients and use the rate of pitch angle diffusion near the loss cone to calculate the timescale for losses τ_L to the atmosphere. Since the magnitude of the mixed diffusion coefficients usually lies between pure pitch angle and pure energy diffusion, the results are most likely to be an underestimate of the increase in flux. Assuming pitch angle isotropy, the evolution of the equatorial energy distribution function $F(E, \alpha_{eq})$ can be obtained by bounce averaging (2) and writing $\langle D_{pp} \rangle$ in terms of the bounce-averaged energy diffusion coefficient $\langle D_{EE} \rangle$ and is given by

$$\left\langle \frac{\partial F}{\partial t} \right\rangle = \frac{\partial}{\partial E} \left[A(E) \langle D_{EE} \rangle \frac{\partial}{\partial E} \left(\frac{F}{A(E)} \right) \right] - \frac{F}{\tau_L}, \quad (9)$$

where

$$A = (E + E_0)(E + 2E_0)^{1/2} E^{1/2}, \quad (10)$$

E is the kinetic energy, $E_0 = m_0 c^2$ is the rest mass energy, and where the last term represents losses to the atmosphere due to wave-particle interactions. The distribution function

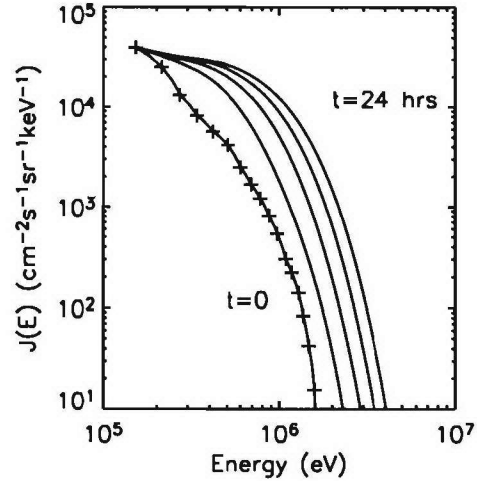


Figure 7. Time evolution of the increase in the electron flux due to whistler mode chorus waves, weighted for latitude and the occurrence of chorus in MLT. The flux is shown at intervals of 6 hours.

$F(E, \alpha_{eq})$ in (9) is a function of energy, not momentum, and is related to the flux $J(E, \alpha_{eq})$ by

$$F(E, \alpha_{eq}) = \frac{A(E)}{c^3} f(\mathbf{p}, \alpha_{eq}) = \frac{(E + E_0)}{c E^{1/2} (E + 2E_0)^{1/2}} J(E, \alpha_{eq}), \quad (11)$$

where we have used $f = J/p^2$. For initial conditions we use the electron flux perpendicular to the ambient magnetic field at $L = 4.5$ measured by the CRRES satellite on 13 October 1990 (orbit 187) during the recovery phase of a magnetic storm [Meredith *et al.*, 2002a, 2002b]. The flux, measured at 18 logarithmically spaced intervals between 0.28 and 1.58 MeV, was interpolated onto a high-resolution regular grid of 500 points between 0.28 and 11 MeV using linear interpolation. The normalized energy diffusion rates ($\langle D_{EE} \rangle / E^2 = 5 \times 10^{-5}$, 1.5×10^{-5} , and $3 \times 10^{-6} \text{ s}^{-1}$) at energies of 100, 300, and 1000 keV, respectively, were also interpolated onto the same high-resolution grid together with the loss timescales obtained from the pitch angle diffusion rates ($\tau_L = p^2 / \langle D_{\alpha\alpha} \rangle = 1.6 \times 10^4$, 5×10^4 , and $2.0 \times 10^6 \text{ s}$). An explicit finite difference method, accurate to second order, was used to solve (9) subject to the condition that the flux at the low- (0.28 MeV) and high-energy boundaries (11 MeV) were kept constant.

[25] The time evolution of the electron flux is shown in Figure 7. In the absence of any other transport processes, the flux > 0.8 MeV increases by more than an order of magnitude and approaches a steady state after about 24 hours where losses balance acceleration. These timescales are comparable to the observed timescale for flux increase in the radiation belts during the recovery phase of magnetic storms [Baker *et al.*, 1986, 1994; Kim and Chan, 1997; Meredith *et al.*, 2002a, 2002b].

7. Discussion

[26] Our results show that there is a competition between electron acceleration and loss for diffusion by whistler mode

chorus waves. Although we have estimated the losses from the pitch angle diffusion coefficients at the edge of the loss cone, a full treatment should take into account the shape of the distribution function in pitch angle and energy. The pitch angle diffusion coefficients are relatively flat near the loss cone and are well below the strong diffusion limit. Therefore we expect that the pitch angle diffusion rates near the edge of the loss cone should give reasonable estimates of the loss rates.

[27] Although losses due to whistler mode chorus are included, losses due to other types of waves, such as plasmaspheric hiss and electromagnetic ion cyclotron (EMIC) waves, have been omitted. Plasmaspheric hiss is mainly confined to within the high-density plasmopause, which is compressed during large geomagnetic disturbances [Meredith *et al.*, 2004]. Since wave acceleration is most efficient in low-density regions, wave acceleration should take place outside the region where hiss dominates. Hiss should contribute to radiation belt losses during the later stages of the recovery phase as the plasmopause expands. Electron losses due to EMIC waves can be significant [Summers and Thorne, 2003; Albert, 2003], but they are generally confined to electron energies greater than ~ 1 MeV [Meredith *et al.*, 2003b]. In addition, EMIC waves are usually confined in MLT to regions close to the plasmopause boundary and therefore electrons would only be scattered during a fraction ($\leq 10\%$) of their drift orbit. Therefore we do not expect these omissions to impact significantly on the main result presented here.

[28] The occurrence of whistler mode chorus in latitude and MLT may have a significant impact on the acceleration of radiation belt electrons. Waves in the prenoon sector dominate energy diffusion above ~ 100 keV. Since these waves occur at latitudes above (and below) the magnetic equator, the diffusion caused by these waves peaks at equatorial pitch angles between 30° and 50° . If pitch angle diffusion is relatively weak, then this could result in butterfly distributions. The results presented here are for conditions averaged over the lifetime of the CRRES orbit, but one may envisage particular storms where, for example, waves at high latitudes in the prenoon sector dominate waves in the night sector. Under these conditions, pitch angle diffusion would be very small for pitch angles greater than about 60° and butterfly distributions should result. Flat-topped pitch angle distributions have been observed during one particular magnetic storm during the recovery phase when the electron flux was observed to increase [Horne *et al.*, 2003a]. These distributions were observed near $L = 4.5$, where magnetopause shadowing can be ruled out and where drift shell splitting should not be significant. We suggest that in addition to drift shell splitting, flat-topped distributions and butterfly distributions could be produced as a result of wave acceleration and could be a signature of wave acceleration. A careful analysis of particle pitch angle distributions in MLT is required to test this suggestion.

8. Conclusions

[29] We have used wave and particle data from the CRRES satellite to determine the timescale for electron acceleration in the heart of the outer radiation belt near $L = 4.5$ due to

whistler mode chorus waves. During magnetically active conditions, we split the wave occurrence into three MLT sectors and determined the contribution to wave acceleration and loss from each sector by calculating the bounce average pitch angle and energy diffusion rates. The results were weighted by the occurrence of the waves in MLT to obtain the timescale for wave acceleration. The main conclusions are as follows:

[30] 1. Chorus wave amplitudes in the night MLT sector peak near the magnetic equator and contribute to significant pitch angle and energy diffusion at pitch angles between 0° and 85° . However, in the prenoon and afternoon MLT sectors chorus wave amplitudes peak at latitudes above and below the magnetic equator. These waves are only effective in causing pitch angle and energy diffusion at equatorial pitch angles less than 60° .

[31] 2. At energies less than ~ 300 keV, there is a competition between electron acceleration and loss to the atmosphere. Above ~ 300 keV, electrons are accelerated faster than they are lost.

[32] 3. After bounce-averaging and weighting the diffusion coefficients by the occurrence of whistler mode chorus in MLT, we find that the timescale for an order of magnitude increase in the electron flux at 1 MeV is about 24 hours at $L = 4.5$. This compares favorably with observations.

[33] 4. We suggest that electron acceleration by whistler mode chorus waves on the dayside of the magnetosphere could produce butterfly pitch angle distributions. Since drift shell splitting becomes small at low L , the best place to determine whether wave acceleration could be responsible for butterfly distributions is at low L during large geomagnetic storms.

[34] We conclude that wave acceleration by whistler mode chorus is a viable mechanism to explain electron flux increases during magnetically disturbed times in the heart of the radiation belts near $L = 4.5$.

[35] **Acknowledgments.** This research was funded in part by the UK Natural Environment Research Council, NASA grant NAG5-11922, and the Space Vehicles Directorate of the Air Force Research Laboratory.

[36] Shadia Rifai Habbal thanks Janet C. Green and Tuija I. Pulkkinen for their assistance in evaluating this paper.

References

- Albert, J. M. (1999), Analysis of quasi-linear diffusion coefficients, *J. Geophys. Res.*, **104**, 2429.
- Albert, J. M. (2003), Evaluation of quasi-linear diffusion coefficients for EMIC waves in a multispecies plasma, *J. Geophys. Res.*, **108**(A6), 1249, doi:10.1029/2002JA009792.
- Albert, J. M. (2005), Evaluation of quasi-linear diffusion coefficients for chorus waves, *J. Geophys. Res.*, A03218, doi:10.1029/2004JA010844.
- Anderson, R. R., D. A. Gurnett, and D. L. Odem (1992), CRRES plasma wave experiment, *J. Spacecr. Rockets*, **29**, 570.
- Baker, D. (2001), Satellite anomalies due to space storms, in *Space Storms and Space Weather Hazards*, edited by I. A. Daglis, pp. 251–284, chap. 10, Springer, New York.
- Baker, D. N., J. B. Blake, R. W. Klebesadel, and P. R. Higbie (1986), Highly relativistic electrons in the Earth's outer magnetosphere: 1. Lifetimes and temporal history 1979–1984, *J. Geophys. Res.*, **91**, 4265.
- Baker, D. N., J. B. Blake, L. B. Callis, R. D. Belian, and T. E. Cayton (1989), Relativistic electrons near geostationary orbit: Evidence for internal magnetospheric acceleration, *Geophys. Res. Lett.*, **16**, 559.
- Baker, D. N., J. B. Blake, L. B. Callis, J. R. Cummings, D. Hovestadt, S. G. Kanekal, B. Klecker, R. A. Mewaldt, and R. D. Zwickl (1994), Relativistic electron acceleration and decay times in the inner and outer radiation belts: SAMPEX, *Geophys. Res. Lett.*, **21**, 409.

- Baker, D. N., et al. (1997), Recurrent geomagnetic storms and relativistic electron enhancements in the outer magnetosphere: ISTP coordinated measurements, *J. Geophys. Res.*, **102**, 14,141.
- Baker, D. N., et al. (1998a), A strong CME-related magnetic cloud interaction with the Earth's magnetosphere: ISTP observations of rapid relativistic electron acceleration on May 15, 1997, *Geophys. Res. Lett.*, **25**, 2975.
- Baker, D. N., T. I. Pulkkinen, X. Li, S. G. Kanekal, J. B. Blake, R. S. Selesnick, M. G. Henderson, G. D. Reeves, H. E. Spence, and G. Rostoker (1998b), Coronal mass ejections, magnetic clouds, and relativistic magnetospheric electron events: ISTP, *J. Geophys. Res.*, **103**, 17,279.
- Baker, D. N., J. H. Allen, S. G. Kanekal, and G. D. Reeves (1998c), Disturbed space environment may have been related to pager satellite failure, *Eos Trans. AGU*, **79**, 477.
- Brautigam, D. H., and J. M. Albert (2000), Radial diffusion analysis of outer radiation belt electrons during the October 9, 1990, magnetic storm, *J. Geophys. Res.*, **105**, 291.
- Elkington, S. R., M. K. Hudson, and A. A. Chan (1999), Acceleration of relativistic electrons via drift resonant interactions with toroidal-mode Pc-5 ULF oscillations, *Geophys. Res. Lett.*, **26**, 3273.
- Friedel, R. H. W., G. D. Reeves, and T. Obara (2002), Relativistic electron dynamics in the inner magnetosphere—A review, *J. Atmos. Sol. Terr. Phys.*, **64**, 265.
- Glauert, S. A., and R. B. Horne (2005), Calculation of pitch angle and energy diffusion coefficients with the PADIE code, *J. Geophys. Res.*, doi:10.1029/2004JA010851, in press.
- Green, J. C., and M. G. Kivelson (2004), Relativistic electrons in the outer radiation belt: Differentiating between acceleration mechanisms, *J. Geophys. Res.*, **109**, A03213, doi:10.1029/2003JA010153.
- Horne, R. B. (2002), The contribution of wave particle interactions to electron loss and acceleration in the Earth's radiation belts during geomagnetic storms, in *Review of Radio Science 1999–2002*, edited by W. R. Stone, pp. 801–828, chap. 33, John Wiley, Hoboken, N. J.
- Horne, R. B. (2003), Rationale and requirements for a European space weather programme, in *Space Weather Workshop: Looking Towards a European Space Weather Programme*, p. 139–144, Eur. Space Agency, ESTEC, Noordwijk, Netherlands.
- Horne, R. B., and R. M. Thorne (1998), Potential waves for relativistic electron scattering and stochastic acceleration during magnetic storms, *Geophys. Res. Lett.*, **25**, 3011.
- Horne, R. B., and R. M. Thorne (2003), Relativistic electron acceleration and precipitation during resonant interactions with whistler-mode chorus, *Geophys. Res. Lett.*, **30**(10), 1527, doi:10.1029/2003GL016973.
- Horne, R. B., N. P. Meredith, R. M. Thorne, D. Heynderickx, R. H. A. Iles, and R. R. Anderson (2003a), Evolution of energetic pitch angle distributions during storm-time electron acceleration to MeV energies, *J. Geophys. Res.*, **108**(A1), 1016, doi:10.1029/2001JA009165.
- Horne, R. B., S. A. Glauert, and R. M. Thorne (2003b), Resonant diffusion of radiation belt electrons by whistler mode chorus, *Geophys. Res. Lett.*, **30**(9), 1493, doi:10.1029/2003GL016963.
- Hudson, M. K., S. R. Elkington, J. G. Lyon, V. A. Machenko, I. Roth, M. Temerin, J. B. Blake, M. S. Gussenhoven, and J. R. Wygant (1997), Simulation of radiation belt formation during sudden storm commencements, *J. Geophys. Res.*, **102**, 14,087.
- Kim, H.-J., and A. A. Chan (1997), Fully adiabatic changes in storm time relativistic electron fluxes, *J. Geophys. Res.*, **102**, 11,107.
- Li, X., and M. A. Temerin (2001), The electron radiation belt, *Space Sci. Rev.*, **95**, 569.
- Li, X., D. N. Baker, M. Temerin, D. Larson, R. P. Lin, G. D. Reeves, M. Looper, S. G. Kanekal, and R. A. Mewaldt (1997), Are energetic electrons in the solar wind the source of the outer radiation belt?, *Geophys. Res. Lett.*, **24**, 923.
- Lyons, L. R. (1974), Pitch angle and energy diffusion coefficients from resonant interactions with ion-cyclotron and whistler waves, *J. Plasma Phys.*, **12**, 417.
- Lyons, L. R., and D. A. Williams (1984), *Quantitative Aspects of Magnetospheric Physics*, Springer, New York.
- Lyons, L. R., R. M. Thorne, and C. F. Kennel (1972), Pitch-angle diffusion of radiation belt electrons within the plasmasphere, *J. Geophys. Res.*, **77**, 3455.
- Meredith, N. P., R. B. Horne, and R. R. Anderson (2001), Substorm dependence of chorus amplitudes: Implications for the acceleration of electrons to relativistic energies, *J. Geophys. Res.*, **106**, 13,165.
- Meredith, N. P., R. B. Horne, D. Summers, R. M. Thorne, R. H. A. Iles, D. Heynderickx, and R. R. Anderson (2002a), Evidence for acceleration of outer zone electrons to relativistic energies by whistler mode chorus, *Ann. Geophys.*, **20**, 967.
- Meredith, N. P., R. B. Horne, R. H. A. Iles, R. M. Thorne, R. R. Anderson, and D. Heynderickx (2002b), Outer zone relativistic electron acceleration associated with substorm enhanced whistler mode chorus, *J. Geophys. Res.*, **107**(A7), 1144, doi:10.1029/2001JA900146.
- Meredith, N. P., M. Cain, R. B. Horne, R. M. Thorne, D. Summers, and R. R. Anderson (2003a), Evidence for chorus driven electron acceleration to relativistic energies from a survey of geomagnetically disturbed periods, *J. Geophys. Res.*, **108**(A6), 1248, doi:10.1029/2002JA009764.
- Meredith, N. P., R. M. Thorne, R. B. Horne, D. Summers, B. J. Fraser, and R. R. Anderson (2003b), Statistical analysis of relativistic electron energies for cyclotron resonance with EMIC waves observed on CRRES, *J. Geophys. Res.*, **108**(A6), 1250, doi:10.1029/2002JA009700.
- Meredith, N. P., R. B. Horne, R. M. Thorne, and R. R. Anderson (2003c), Favored regions for chorus-driven electron acceleration to relativistic energies in the Earth's outer radiation belt, *Geophys. Res. Lett.*, **30**(16), 1871, doi:10.1029/2003GL017698.
- Meredith, N. P., R. B. Horne, R. M. Thorne, D. Summers, and R. R. Anderson (2004), Substorm dependence of plasmaspheric hiss, *J. Geophys. Res.*, **109**, A06209, doi:10.1029/2004JA010387.
- Miyoshi, Y., A. Morioka, T. Obara, H. Misawa, T. Nagai, and Y. Kasahara (2003), Rebuilding process of the outer radiation belt during the November 3, 1993, magnetic storm: NOAA and EXOS-D observations, *J. Geophys. Res.*, **108**(A1), 1004, doi:10.1029/2001JA007542.
- O'Brien, T. P., K. R. Lorentzen, I. R. Mann, N. P. Meredith, J. B. Blake, J. F. Fennel, M. D. Looper, D. K. Milling, and R. R. Anderson (2003), Energization of relativistic electrons in the presence of ULF power and MeV microbursts: Evidence for dual ULF and VLF acceleration, *J. Geophys. Res.*, **108**(A8), 1329, doi:10.1029/2002JA009784.
- Olsen, W. P., and K. Pfizter (1977), Magnetospheric magnetic field modeling, *Annu. Sci. Rep. F44620-75-c-0033*, Air Force Off. of Sci. Res., Bolling Air Force Base, Washington, D. C.
- Reeves, G. D., K. L. McAdams, R. H. W. Friedel, and T. P. O'Brien (2003), Acceleration and loss of relativistic electrons during geomagnetic storms, *Geophys. Res. Lett.*, **30**(10), 1529, doi:10.1029/2002GL016513.
- Schulz, M., and L. Lanzerotti (1974), *Particle Diffusion in the Radiation Belts*, Springer, New York.
- Singer, H. J., W. P. Sullivan, P. Anderson, F. Mozer, P. Harvey, J. Wygant, and W. McNeil (1992), Fluxgate magnetometer instrument on the CRRES, *J. Spacecr. Rockets*, **29**, 599.
- Stix, T. H. (1992), *Waves in Plasmas*, Am. Inst. of Phys., New York.
- Summers, D., and R. M. Thorne (2003), Relativistic electron pitch-angle scattering by electromagnetic ion cyclotron waves during geomagnetic storms, *J. Geophys. Res.*, **108**(A4), 1143, doi:10.1029/2002JA009489.
- Summers, D., R. M. Thorne, and F. Xiao (1998), Relativistic theory of wave-particle resonant diffusion with application to electron acceleration in the magnetosphere, *J. Geophys. Res.*, **103**, 20,487.
- Summers, D., C. Ma, N. P. Meredith, R. B. Horne, R. M. Thorne, D. Heynderickx, and R. R. Anderson (2002), Model of the energization of outer-zone electrons by whistler-mode chorus during the October 9, 1990 geomagnetic storm, *Geophys. Res. Lett.*, **29**(24), 2174, doi:10.1029/2002GL016039.
- Summers, D., C. Ma, N. P. Meredith, R. B. Horne, R. M. Thorne, and R. R. Anderson (2004), Modeling outer-zone relativistic electron response to whistler mode chorus activity during substorms, *J. Atmos. Sol. Terr. Phys.*, **66**, 133.
- J. M. Albert, Air Force Research Laboratory/VSBX, 29 Randolph Road, Hanscom AFB, MA 01731-3010, USA. (jay.albert@hanscom.af.mil)
- R. R. Anderson, Department of Physics and Astronomy, University of Iowa, Iowa City, IA 52242-1479, USA. (roger-r-anderson@uiowa.edu)
- S. A. Glauert and R. B. Horne, British Antarctic Survey, Natural Environment Research Council, Madingley Road, Cambridge CB3 0ET, UK. (sagl@bas.ac.uk; r.horne@bas.ac.uk)
- N. P. Meredith, Mullard Space Science Laboratory, University College London, Holmbury St. Mary, Dorking RH5 6NT, UK. (npm@mssl.ucl.ac.uk)
- R. M. Thorne, Department of Atmospheric Sciences, University of California, Los Angeles, 405 Hilgard Avenue, Los Angeles, CA 90095-1565, USA. (rmt@atmos.ucla.edu)